# Sensor Calibration Errors in Compressive Distributed-Aperture Radar Sensing

Peter B. Tuuk, Amy C. Sharma
Georgia Tech Research Institute
Sensors and Electromagnetic Applications Laboratory
Atlanta, GA 30332
{peter.tuuk, amy.sharma}@gtri.gatech.edu

***Abstract*—As unmanned platforms become more common, the desire for lightweight, low-power, inexpensive radar systems has increased. The impact of sensor calibration errors on a distributed-aperture radar utilizing compressed sensing techniques is explored herein. We developed a model to derive performance curves for detection of targets in range-angle-Doppler space using a number of single element radar transmitters/receivers versus the accuracy to which the locations of these sensors are known and the precision to which the system can be time-synchronized. Our results show that the compressed sensing process is not brittle with respect to modeling errors of this type.**

***Index Terms*—Multiple Input Multiple Output Radar; Compressed Sensing; Modeling Error**

## I. Introduction

THE RECENT dawn of unmanned platforms has given new impetus to the desire for lightweight, low-power, inexpensive radar systems to provide capabilities once found only on high-end platforms. Toward this goal we investigate the feasibility of a distributed-aperture radar system that uses compressed sensing concepts to lower the system communications throughput. Of particular interest is the performance of such a system in the presence of sensor position and temporal synchronization uncertainty.

### A. Motivation

We investigate the feasibility of using multiple simple elements cooperatively to form a coherent MIMO radar array. This concept has many attractive features:

*1) Improved Resolution:* Results showing that distributed-aperture radar achieves improved resolution come out of research in the field of multiple-input, multiple-output (MIMO) radar. In a MIMO construct, the radar designer eschews the traditional high correlation of waveforms from one element to the next. Rather than steering the beam in a particular direction by phase-shifting or time-delaying, the MIMO radar elements transmit independent waveforms. MIMO radar systems typically fall into two categories: uncorrelated and correlated.

In the uncorrelated case, widely separated antennas enjoy independent looks at the target. Since the target radar cross section (RCS) function decorrelates with aspect angle, these widely-spaced looks are exploited to reduce scintillation and improve detection performance over the monostatic baseline [1]. Given the uncorrelated target responses, optimal detection necessitates summing of the target responses in magnitude only.

Correlated MIMO radar, by contrast, does not assume or exploit diversity in look-angle or target RCS. Rather the transmitters and receivers are located close to one another relative to the target. These transmitters and receivers act as a coherent virtual array formed by the spatial convolution of the transmit and receive arrays, increasing the effective aperture size. In this case, the MIMO radar achieves an improvement in angular resolution relative to a classical phased array radar with the same number of elements [2]. It is on this second, correlated, case that we focus our attention.

*2) Simple Sensors:* Since each platform in the formation need only act as one element in a larger array, the sensing systems aboard each platform need not possess the native complexity of a radar developed for independent employment. In particular the beam pattern of each sensor may (and, in fact, *must*) be very broad in angle. Since angular resolution is proportional to the radio frequency (RF) wavelength divided by the aperture width [3]

$$\Delta_\theta \propto \frac{\lambda}{D_\theta} \tag{1}$$

it can be difficult to achieve useful resolution at lower frequencies on a low-cost, small platform.

By using a formation cooperatively the aperture width can be increased beyond the size of any one platform. This wide aperture can produce useful angular resolution at lower frequencies of interest. But since each antenna is itself only an element in the larger aperture these sensors can be made with very few radiating elements. Whereas a multifunction airborne radar may have thousands of phase-steered elements, the wide beam-pattern (really the pattern of an element in the larger MIMO array) of these simple antennas means they may have very few.

*3) Scalable Performance:* Another advantage of such a system is the flexibility it gives to the operator. Theory predicts and our simulation results confirm that performance increases with both number of elements and formation size. Thus an inventory of available platforms can be allocated to various tasks; each lends detection performance, resolution, and usable power as necessitated by the importance or requirements of the task at hand.

### B. Challenges

But all these attractive features come with some notable challenges as well. Communication demands are immense. All measurements must be passed to a fusion center which processes all in-phase & quadrature data. Total system communication throughput required is the product of number of elements, pulse repetition frequency, number of samples per pulse, and quantization bits. Additionally, achieving usable system synchronization in this sensing structure is difficult.

Therefore we use compressed sensing acquisition to reduce the communication demands and we test the performance of this technique in the presence of model errors arising from sensor position and time synchronization errors across platforms.

### C. Paper Organization

The remainder of this paper is organized as follows: Section II introduces the relevant concepts of compressed sensing, Section III details the experimental setup and method, Sections IV and V describe the results of these and summarize the impact thereof.

## II. Compressed Sensing

### A. Theory

To coherently process all measurements made at all sensors would require immense communications throughput. Compressed sensing (CS) techniques, however, offer hope for capability with fewer measurements.

CS results show that sparse signals can be reconstructed from fewer measurements than would otherwise be required under classical sampling paradigms [4]–[6]. This depends on the sparsity of the signal to be acquired as well as the basis used to measure it.

Some signal $\mathbf{x} \in \mathbb{C}^m$ is $s$-sparse if at most $s$ of its $m$ elements are non-zero. Measurements $\mathbf{y} \in \mathbb{C}^n$ of $\mathbf{x}$ are modeled by applying the linear operator $\mathbf{A} \in \mathbb{C}^{n \times m}$ so that $\mathbf{y} = \mathbf{A}\mathbf{x}$. To reconstruct $\mathbf{x}$ accurately, the measurement operator must collect measurements in a way that is uncorrelated with the signal's sparsifying basis [6]. This condition is satisfied with high probability in the case of random measurement operators.

Such measurements can be used to estimate $\mathbf{x}$ by solving the convex optimization problem

$$\hat{\mathbf{x}} = \arg\min_{\mathbf{x}} ||\mathbf{x}||_1 \ \text{ s.t. } \ \mathbf{y} = \mathbf{A}\mathbf{x}. \tag{2}$$

Similarly in the presence of noise a relaxed version of this problem can be solved:

$$\hat{\mathbf{x}} = \arg\min_{\mathbf{x}} ||\mathbf{x}||_1 \ \text{ s.t. } \ ||\mathbf{y} - \mathbf{A}\mathbf{x}||_2^2 \leq \varepsilon. \tag{3}$$

### B. Practice

*1) Realizable CS Receivers:* Applications of these ideas are becoming reality. Because acquiring measurements according to random projections in time is challenging from a hardware perspective, other methods must be developed. One way to acquire useful measurements is to follow a mix, filter, and downsample paradigm [7]. The incoming signal is mixed with a pseudo-random (but known) signal before being low-pass filtered and sampled. The pseudo-random mixing signal must have a high bandwidth but the subsequent sampling may be much slower. This mix-filter-downsample process spreads the signal energy in a way that enough information is present in the narrow sampled band to estimate $\mathbf{x}$. Such samplers will act as the receiver elements of the simulated radar system.

*2) Presence of Sparsity:* Compressed sensing results depend on sparsity in the signal to be measured. In most radar search functions target locations can be sparely represented in the observation space. In the radar field of view there may be only a handful of targets. These targets could be missiles cresting the horizon in a surveillance radar or moving vehicles in a ground moving target indicator system. The nature of the search function implies that most potential target locations are empty.

## III. Method

To test our hypotheses about the performance and robustness of the postulated distributed-aperture radar system we develop a simulation framework in which targets, measurements, and modeling errors can be represented.

### A. Geometry

First, flatten the world into a two-dimensional plane. The scenario under investigation involves $n_{e_t}$ radar transmit elements and $n_{e_r}$ receive elements (that may be co-located) randomly situated in a disk of radius $\rho$ around the origin with a uniform polar distribution. Place the $i$-th transmitter at radius $r_{t_i} \in [0, \rho]$ and angle $\theta_{t_i} \in [0, 2\pi)$. Similarly, place the $i$-th receiver at radius $r_{r_i} \in [0, \rho]$ and angle $\theta_{r_i} \in [0, 2\pi)$.

### B. Pulses

The $i$-th transmitter produces the radio frequency (RF) pulse as a function of time $p_i(t)$ that illuminates the entire angular observation space uniformly. Element beam-pattern effects are neglected in this analysis.

The pulses from all $n_{e_t}$ transmitters sum coherently in different ways as a function of the transmission angle, thus we define the effective pulse of this sparse array as a function of transmission angle: $p_e(\theta, t)$. Assuming the range to the area under observation is much greater than $\rho$, the effective pulse at angle $\theta$ can be expressed as

$$p_e(\theta, t) = \sum_{i=1}^{n_{e_t}} p_i(t - \cos(\theta - \theta_{t_i}) r_{t_i}/c) \tag{4}$$

where $c$ is the speed of light. This geometry and problem formulation builds on work presented in [8].

### C. Target Returns

The $i$-th target, located in range-angle-Doppler space at $(r_{x_i}, \theta_{x_i}, d_{x_i})$ with complex radar cross-section $\chi_i$, is illuminated by the effective pulse $p_e(\theta_{x_i}, t - r_{x_i}/c)$. It reflects energy back to the receivers delayed according to its range and frequency-shifted according to its radial velocity.

While the total target return at the origin is

$$p_r(t) = \sum_{i=1}^{n_t} \chi_i p_e \left( \theta_{x_i}, t - \frac{2 r_{x_i}}{c} \right) e^{2\pi j d_{x_i}} \tag{5}$$

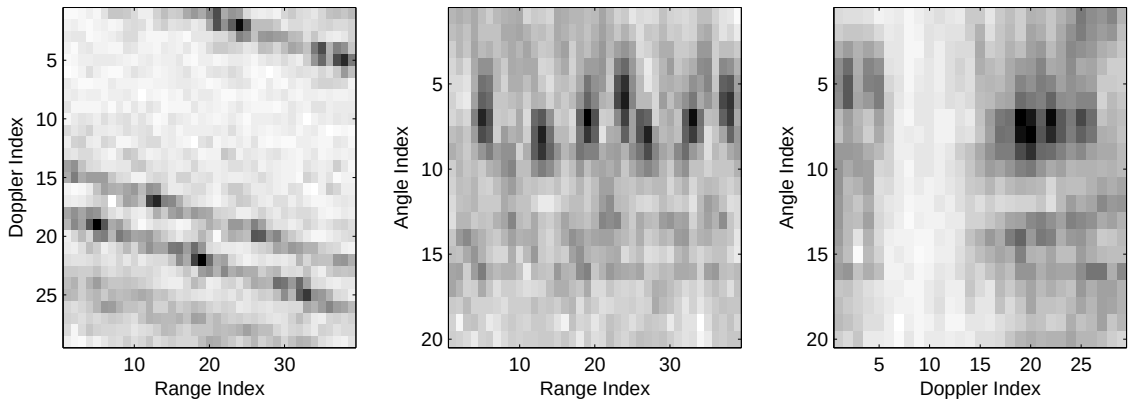


Fig. 1: Target response from matched filter reconstruction using LFM pulse in Range-Doppler, Range-Angle, and Doppler-Angle slices. Characteristic range-Doppler coupling sidelobes features prominently in the range-Doppler view. This reconstruction is made with uncompressed measurements according to $\hat{\mathbf{x}} = \mathbf{B}^{\mathrm{H}}\mathbf{B}\mathbf{x}$ following the notation in (7).

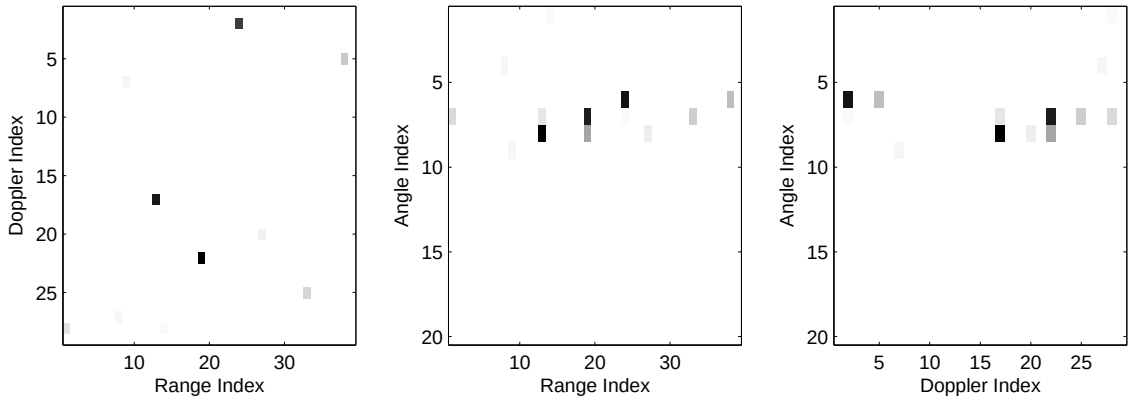


Fig. 2: Target response from relaxed $\ell_1$ reconstruction using LFM pulse in Range-Doppler, Range-Angle, and Doppler-Angle slices. Sparsity of the target indicator vector is evident, though sidelobes present some challenge to the reconstruction algorithm when using the LFM pulse.

the return at the receiver locations will vary. Assuming the targets are far from the sensors relative to $\rho$, as in (4), the return to receiver $k$ over time is

$$p_{r_k}(t) = \sum_{i=1}^{n_t} \chi_i p_e\left(\theta_{x_i}, t - \frac{2r_{x_i} - \cos(\theta_{x_i} - \theta_{r_k})r_{r_k}}{c}\right) e^{2\pi j d_{x_i}}. \tag{6}$$

### D. Forward Operator

In order to solve the problem presented in Section I by those techniques referred to in Section II, one must model the distributed-aperture radar system with a linear operator. Development of the forward operator is an exercise in listing. The forward operator, $\mathbf{A}$ in $\mathbf{y} = \mathbf{A}\mathbf{x}$, is a dictionary of returns from targets at each gridded location in the search space.

This process can be split into two independent operators. The first, $\mathbf{B}$, describes the geometry and waveforms through which the locations and intensities of the targets are observed by the receivers. The structure along the range dimension is Toeplitz, the structure in the angle dimension is captured by the angle-variation of the effective pulse $p_e(\theta, t)$, and the Doppler dimension is generated by making frequency-shifted copies of the range-angle sub-operator. The full set of measurements that could be taken at the receivers is $\mathbf{B}\mathbf{x}$ which is the over-sample data cube.

Figure 1 shows an example target response from three targets in the observation space. The three non-zero elements in $\mathbf{x}$ are mapped through $\mathbf{B}$ onto the observations. The matched filter is then applied to the returns to generate the observed response $\hat{\mathbf{x}} = \mathbf{B}^{\mathrm{H}}\mathbf{B}\mathbf{x}$ (following the notation in (7)). The undersampling in the spatial is evident in the multiple sidelobes that accompany each real target.

The second operator, $\mathbf{C}$ represents the sampling operations that occur at each of the receivers to make the compressive measurements. It is in $\mathbf{C}$ that the mix-filter-sample operation of [7] is represented. The mixing operation is represented by a diagonal matrix, filtering by a Toeplitz matrix, and sampling by an identity matrix in which most of the rows are removed, leaving only those samples that are to be stored. The product

of these three matrices is $\mathbf{C}$. Finally

$$\mathbf{y} = \mathbf{CBx} = \mathbf{Ax} \tag{7}$$

are those measurements that are made and processed for target detection.

Figure 2 shows the relaxed $\ell_1$ reconstruction of three targets using compressive measurements made according to (7). The comparison between Figures 1 and 2 shows the sparse nature of solutions obtained by compressed sensing techniques.

### *E. Errors*

Thermal noise, $\mathbf{e}$, in the receivers of a radar system can be modeled as an independent Gaussian contribution to the measurements $\mathbf{y} = \mathbf{Ax} + \mathbf{e}$. Much work in compressed sensing has focused on performance of measurement designs and reconstruction algorithms in the presence of such noise.

Clutter, $\mathbf{c}$, enters the measurements differently as it is correlated with the transmitted pulse $\mathbf{y} = \mathbf{A}(\mathbf{x} + \mathbf{c}) + \mathbf{e}$. Reducing clutter is more challenging than reducing noise since clutter scales with the power of the transmitted pulse and responds to the same matched filter that brings targets out of white noise.

Sensor calibration errors introduce an error to the measurement operator $\mathbf{A}$ as in [9]. If the operator based on perceived element locations is $\hat{\mathbf{A}}$ but the operator based on truth is $\mathbf{A}$ then $\hat{\mathbf{A}} = \mathbf{A} + \mathbf{E}$ and

$$\mathbf{y} = (\hat{\mathbf{A}} - \mathbf{E})\mathbf{x}. \tag{8}$$

To simulate the effect of model errors, we introduce a time and position error at each sensor. The position error at each sensor was modeled as normally distributed two-dimensional random variable with standard deviation $\sigma_l$ in each dimension. We consider sensor position errors relative to the wavelength of the RF transmissions, $\lambda$. Likewise timing errors were modeled as a normally distributed random variable at each sensor with mean 0 and standard deviation $\sigma_t$. These errors are relative to the time it takes a pulse to travel one RF wavelength: $\lambda/c$.

We then apply the true $\mathbf{A}$ to some scene $\mathbf{x}$ to generate measurements which are fed into a reconstruction algorithm that assumes the measurement model $\hat{\mathbf{A}}$. In our case the reconstruction method is the Sparse Reconstruction by Separable Approximation algorithm proposed in [10] with debiasing and safeguards enabled.

## IV. Results

Our interest lies in the ability of a system as described in Section I to detect targets. To evaluate that performance we must decide on some detection criteria. Sparsity, assumed in compressed sensing and induced by the relevant reconstruction methods, renders moot much of the successful body of practice that has developed around radar target detection. Constant false-alarm rate (CFAR) detectors and much of classical Neyman-Pearson theory are not directly applicable. For this reason, we use a naïve detector that selects as a detection any cell with an amplitude greater than $1/10$ (normalized by maximum target amplitude).

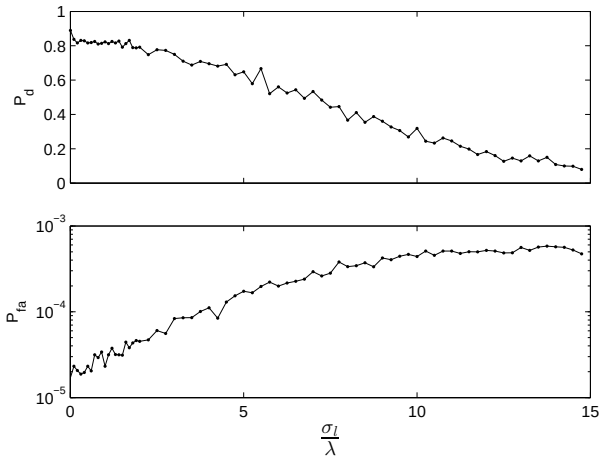


(a) Location Errors: $P_d$ and $P_{fa}$ vs. $\sigma_l/\lambda$

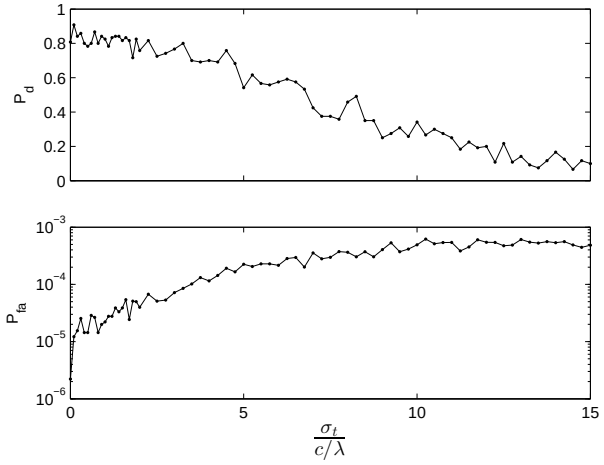


(b) Time Synchronization Errors: $P_d$ and $P_{fa}$ vs. $\sigma_t/\frac{c}{\lambda}$

Fig. 3: These two figures demonstrate the similarity of errors in time and space for genereating detection errors. When normalized according to the wavelength both error modalities are manifest in similar detection error curves.

Variables that drive detection performance in this problem formulation include signal-to-noise ratio (SNR), signal-to-clutter ration (SCR), sub-sampling factor at the compressive analog to digital convertor, number of radiating and receiving elements, size of element-containing disk, number of targets, and sensor calibration errors. To explore the high-dimensional parameter space Monte Carlo methods were used to estimate expected performance over rays through this space.

The first of these experiments demonstrates the fall-off in detection performance as system calibration errors increase. Figures 3(a) and 3(b) show the effect of location and time synchronization errors on the ability to detect targets and reject false targets. For these results we used a 5 dB signal-to-noise ratio, a 5 dB signal-to-clutter ratio, a sampling speed $1/16$ of the Nyquist rate, 7 transmitter/receivers elements, and 3 targets randomly situated in a search space around 23 000 bins.

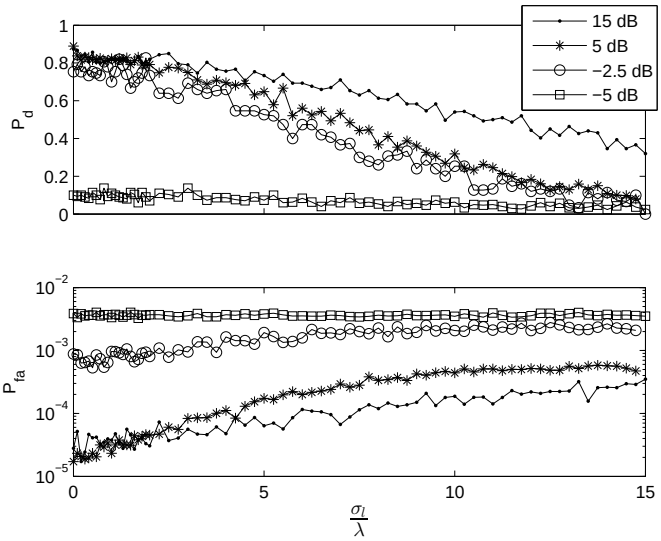


Fig. 4: $P_d$ and $P_{fa}$ vs. $\sigma_l/\lambda$ for various SNR

Simulation shows that as sensor location error increases, the probability of detection ($P_d$) decreases and the probability of false alarm ($P_{fa}$) increases as illustrated in Figure 3(a). Another case of modeling error is time synchronization error. Simulation results displayed in Figure 3(b) show that the performance degradation due to this is virtually identical to the effect of position error (when both are normalized appropriately) even though the two errors accumulates differently with respect to the various elements.

The second set of results, in Figure 4, shows the effect of noise power on the detection performance vs. system synchronization curves. Here we use the same set of parameters as in Figure 3 but vary the SNR. Predictably, increasing the noise level decreases performance but the impact on is not constant. With small synchronization errors noise power does not strongly impact probability of detection of targets but does greatly diminish false-alarm performance. With large synchronization errors only in the very high SNR case is any detection possible.

## V. Conclusion

This work helps to bound the feasible region of employ for a system as described in Section I. Our results show that performance in off-nominal system synchronization cases does not suddenly evaporate. Rather, the system architect can balance required detection performance, available signal-to-noise ratio, and system synchronization complexity to find a successful balance.

Future work will involve comparison to theoretical bounds, improved waveform design, detection criteria tailored to the specific distributions produced by these techniques, and clutter mitigation techniques integral to the sparse solution process.

## References

[1] A. Haimovich, R. Blum, and L. Cimini, "MIMO radar with widely separated antennas," *Signal Processing Magazine, IEEE*, vol. 25, pp. 116–129, Jan. 2008.

[2] J. Li and P. Stoica, "MIMO radar with colocated antennas," *Signal Processing Magazine, IEEE*, vol. 24, pp. 106–114, Sept. 2007.

[3] M. A. Richards, *Fundamentals of Radar Signal Processing*. New York: McGraw-Hill, 2005.

[4] E. J. Candès, J. K. Romberg, and T. Tao, "Stable signal recovery from incomplete and inaccurate measurements," *Communications on Pure and Applied Mathematics*, vol. 59, no. 8, pp. 1207–1223, 2006.

[5] D. Donoho, "Compressed sensing," *Information Theory, IEEE Transactions on*, vol. 52, no. 4, pp. 1289–1306, 2006.

[6] E. Candès and J. Romberg, "Sparsity and incoherence in compressive sampling," *Inverse Problems*, vol. 23, no. 3, pp. 969–985, 2007.

[7] J. Tropp, J. Laska, M. Duarte, J. Romberg, and R. Baraniuk, "Beyond Nyquist: Efficient sampling of sparse bandlimited signals," *Information Theory, IEEE Transactions on*, vol. 56, pp. 520–544, Jan. 2010.

[8] Y. Yu, A. Petropulu, and H. Poor, "MIMO radar using compressive sampling," *Selected Topics in Signal Processing, IEEE Journal of*, vol. 4, no. 1, pp. 146–163, 2010.

[9] M. Herman and T. Strohmer, "General deviants: An analysis of perturbations in compressed sensing," *Selected Topics in Signal Processing, IEEE Journal of*, vol. 4, no. 2, pp. 342–349, 2010.

[10] S. Wright, R. Nowak, and M. Figueiredo, "Sparse reconstruction by separable approximation," *Signal Processing, IEEE Transactions on*, vol. 57, pp. 2479–2493, July 2009.